Updating the low-frequency model in time-lapse seismic inversion: A case study from a heavy-oil steam-injection project

Peter R. Mesdag[1], M. Reza Saberi[1], and Cheran Mangat[2]

Abstract

A workflow to update the time-lapse low-frequency model in a data-driven manner in time-lapse inversion studies is applied to a heavy-oil reservoir produced using the steam-assisted gravity drainage (SAGD) method. The base seismic survey and the difference between the base and monitor surveys are inverted in two separate inversion runs, and no assumptions are made regarding the reservoir changes or the relationships between elastic or reservoir parameters. The effects of production are estimated from the inversion of the difference between the base and monitor surveys. This information is used to update the low-frequency model in the time-lapse sense. A good match can be observed between the inversion results and other available information from the field, confirming the validity of the method.

Introduction

Time-lapse seismic reservoir monitoring is a common and powerful methodology for mapping the changes in subsurface reservoirs resulting from production. In our approach, mapping these changes requires three main phases. The first phase, which is the subject of this article, is the inversion of time-lapse seismic data to estimate the changes in elastic parameters caused by production. The method described for this phase can be seen as a 4D extension to a 3D method for updating the low-frequency model described by Mesdag et al. (2010). Independent measures are obtained of time-lapse absolute P-impedance and time-lapse absolute V_P/V_S (or $\lambda\rho$, multiplication of lambda and density, and $\mu\rho$, multiplication of shear modulus and density). These parameters then can be compared with propagation parameters such as 4D time shifts or velocity changes.

The second phase of the workflow is the integration of all available data from independent disciplines such as petrophysics, seismic, reservoir, and production engineering to derive a consistent model in which a general rock-physics relationship can help to fill in missing information in any of these four disciplines over the entire field. Saberi et al. (2015) describe the workflow of this second phase and derive a rock-physics template for the heavy oil reservoir studied here.

In the third and last phase, this rock-physics template is used to interpret time-lapse inversion results in terms of steam chambers and reservoir temperatures. An example of the third phase is illustrated at the end of this article, where the results of the time-lapse inversion are mapped into reservoir properties (temperature changes, in this case) using the petroelastic model derived in phase two, and the temperature images are compared against any available wells with temperature well logs within the study area.

Case study and data preparation

The production of dense and viscous oils at low temperature can be facilitated by using enhanced oil-recovery methods such as steam-assisted gravity drainage (SAGD), in which the temperature of the reservoir is increased by the injection of hot, pressurized steam. This operation creates steam chambers where oil viscosity is reduced, and the bitumen is forced to flow into the production wells at the base of these chambers.

Time-lapse inversion can be quite useful for quantifying production parameters such as temperature and pressure or the development and extent of the steam chambers, which usually can reach 40 to 50 m in thickness. The conventional seismic signal used to investigate such shallow-depth reservoirs is generally high frequency and has limited power at low frequencies, resulting in an extracted wavelet of short period with a dominant wavelength of about 30 m (20 ms).

Lacking the low-frequency component, the seismic data will contain only part of the information necessary to characterize the reservoir. Much of the information will have to come from the time-lapse low-frequency response of the subsurface. Rock-physics models can be used to update the low-frequency model at well control, but away from wells, seismic data might be the only information available.

The available data in our case study are prestack seismic data from the base and monitor surveys as well as elastic logs for some drilled wells inside the field. The first step is the preparation of the available data for time-lapse inversion. Data equalization and time alignment are the two important steps to address seismic data preparation, whereas well-log preparation and correction can be dealt with through rock-physics modeling (Saberi et al., 2015).

Data equalization normally is applied based on measurements from an area above the reservoir section where no time-lapse changes are expected. This area provides a good estimate of the repeatability of the data between the base and monitor seismic surveys and should be used to extract attributes for data equalization between vintages, such as root-mean-square (rms) of the seismic amplitudes over a time window. If any changes are observed in the base and monitor attributes, these probably are caused by differences in the acquisition between base and monitor surveys. These acquisition-induced differences are likely to be pervasive throughout the seismic trace and if not addressed, will cause false time-lapse effects within the reservoir.

Figure 1 depicts this equalization process in four images. The rms is extracted within the overburden for both the base and monitor surveys as shown in Figures 1a and 1b, respectively. The monitor survey is scaled to the base survey through a correction factor shown in Figure 1c, that is calculated from the aforementioned rms extractions.

[1]CGG.
[2]APEGA.

http://dx.doi.org/10.1190/tle34121456.1.

The next step of data preparation is to address the time difference between the base and monitor surveys through a time-alignment procedure. Most inversion techniques do not account for such a misalignment of seismic reflectivity during the inversion process. Therefore, any misalignment needs to be removed prior to seismic inversion. In the case of prestack inversion (the inversion technique used in this article), the alignment needs to be applied both in the offset, or angle, direction and in the time-lapse direction.

In SAGD, the time shifts between base and monitor surveys are generally considerable. Time shifts can be calculated in many ways, but for relatively small time shifts, crosscorrelation between the two surveys usually gives satisfactory results. Note that time shifts associated with low crosscorrelation need to be avoided.

Figure 2 depicts a method to achieve this in which a combination of crosscorrelation and the time-shift values is captured by a polygon and used as a threshold to blank out any dubious time shifts. Prior to applying the time shifts, the undefined values are interpolated in a 3D sense.

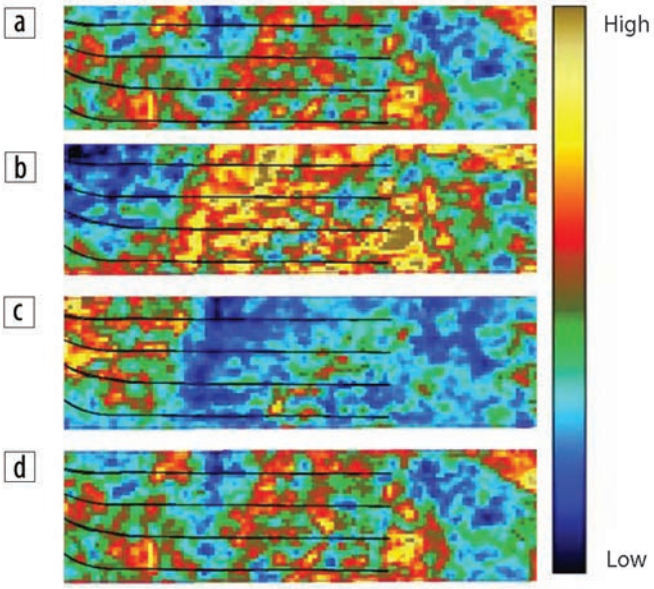

Figure 1. (a) rms seismic attribute extracted from the baseline seismic survey. (b) rms seismic attribute extracted from the monitor seismic survey. (c) Correction factor calculated from base and monitor rms extractions. (d) rms extraction from monitor after correction. The correction factor shown in (c) expresses the rms difference in the overburden between the base and monitor acquisitions.

Time-lapse inversion

The most common 4D inversion workflows known to the industry include either a separate inversion of the base and monitor surveys (e.g., Sarkar et al., 2003) or a simultaneous inversion of the base and monitor, as illustrated, for instance, by Michou et al. (2013) in the framework of an onshore permanent reservoir monitoring.

The 4D inversion workflow used in this study is composed of four steps:

- Step 1: Full-bandwidth prestack inversion of the base survey to provide full-bandwidth inversion models of the reservoir at original conditions.

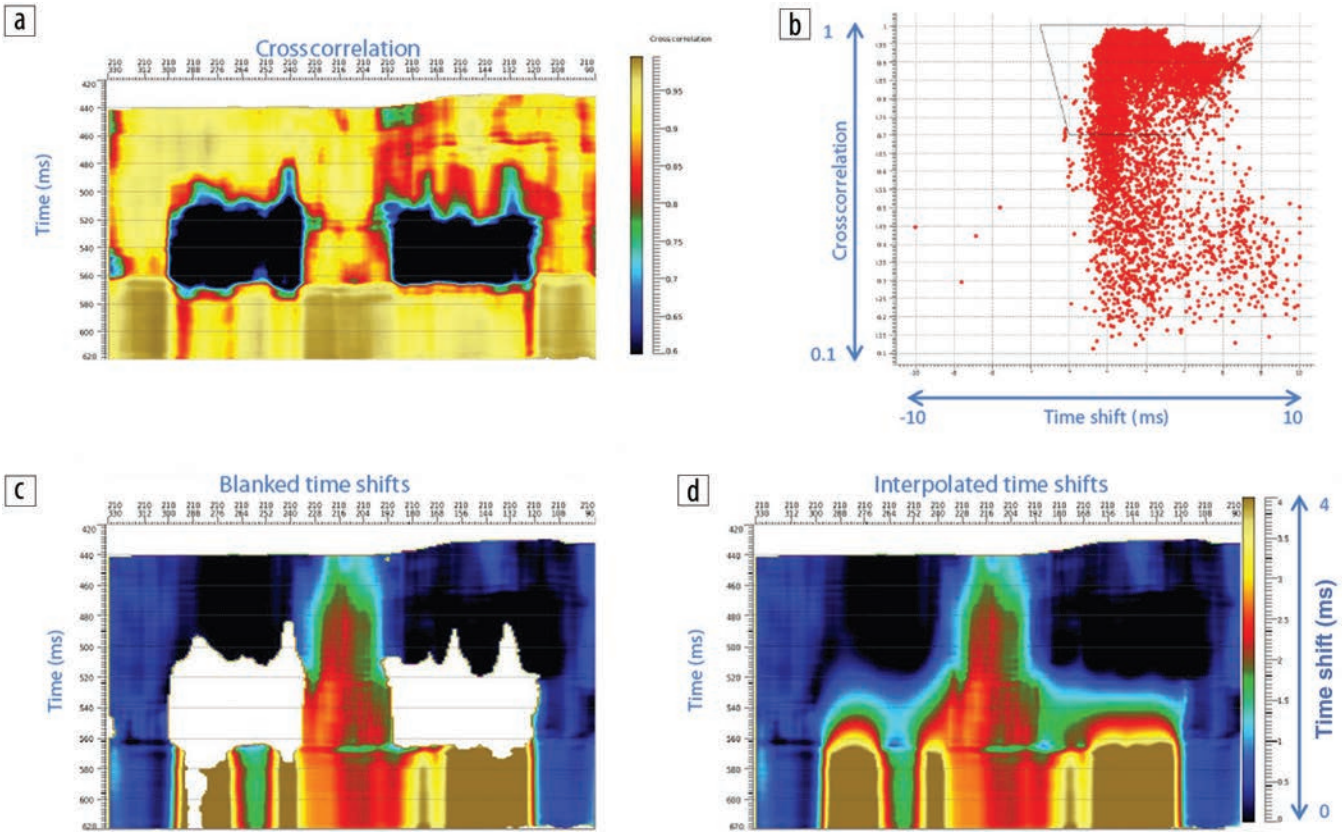

Figure 2. Procedure for monitor-to-base time alignment depicting (a) crosscorrelation, (b) crossplot with a polygon outside of which the time shifts are discarded, (c) blanked time shifts, and (d) interpolated time shifts.

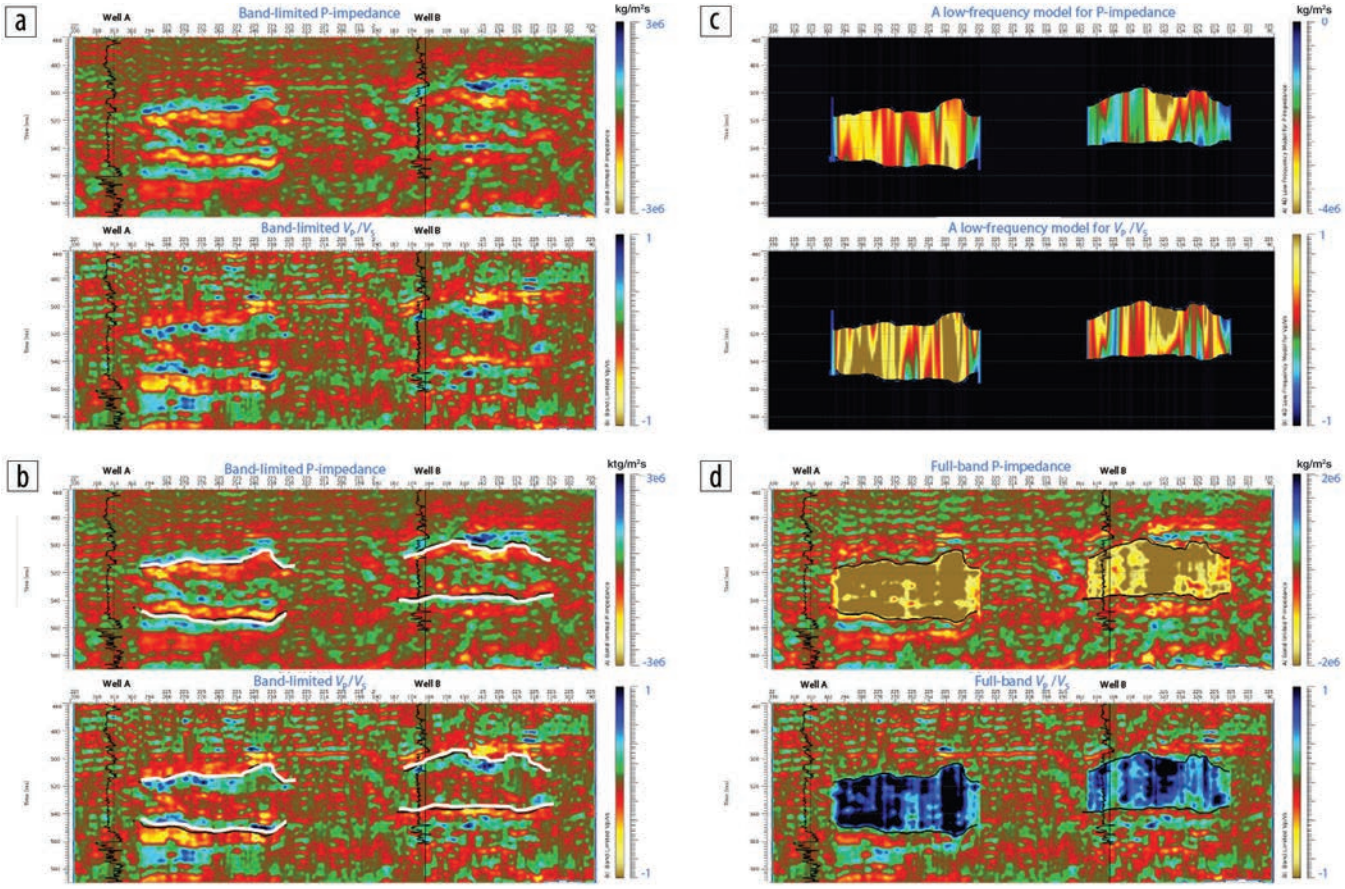

Figure 3. Time-lapse inversion workflow to update the low-frequency model. (a) Band-limited time-lapse P-impedance and V_P/V_S. (b) Same as (a) with the interpreted tops and bases of the steam chambers shown. (c) Low-frequency models for P-impedance and V_P/V_S. (d) Full-bandwidth P-impedance and V_P/V_S after merging with the constructed low-frequency models. Note that black in part (c) refers to places where the elastic properties are not affected by production and are assigned a zero value.

- Step 2: Inversion of the seismic differences to delineate the steam chambers (volumes where production effects are observed and the low-frequency model needs to be adjusted).
- Step 3: Construction of time-lapse low-frequency models to account for production effects.
- Step 4: Merging of the time-lapse low-frequency models from step 3 into the time-lapse inversion models from step 2 to create final full-bandwidth time-lapse models.

In step 1, we perform a simultaneous inversion of the partial stacks of the base survey to build a 3D full-bandwidth model of both P-impedance and V_P/V_S. The low-frequency trends used in this inversion are obtained by interpolation of low-pass filtered well logs within a structural framework based on the interpreted horizons.

In step 2, we perform a simultaneous inversion on the differences between the partial stacks of the monitor and base seismic vintages. These differences are calculated after the application of the equalization and time-shift alignment as described above. To justify inverting the differences rather than the base and monitor surveys themselves, we need to make the assumption that the time-lapse reflection coefficients are small and thus linearly related to the changes in the elastic parameter contrasts. Because the time-lapse changes in reflection coefficients are an order of magnitude smaller than the regular 3D reflection coefficients, it is reasonable to assume they are small.

The 3D models from the inversion of the base survey in step 1 are used directly as the background trends for the time-lapse inversion in step 2. The results of step 2 are then low-cut filtered to remove the 3D, nonupdated trends and produce a band-limited time-lapse P-impedance and a band-limited time-lapse V_P/V_S. Figure 3a shows sections of these band-limited results for our case study. Together, steps 1 and 2 correspond to what we call the "first-pass time-lapse inversion process."

The band-limited time-lapse P-impedance and time-lapse V_P/V_S cubes generated in step 2 are used to pick the tops and bases of the reservoir zones affected by production. This is a straightforward procedure because wherever the time-lapse signal does not show a clear response, the production is not affecting the elastic parameters in that part of the reservoir and the low-frequency model remains unchanged. In many cases, the interpretation can be done by automatic picking, although for the weaker and ambiguous interpretations, interpretive knowledge is essential.

The interpretation of the top and base of the steam chambers should be placed at the zero crossing between a maximum and a minimum of either or both of the elastic parameters. In some areas, one might not see a P-impedance response, whereas in other areas, the time-lapse V_P/V_S changes might be small. If neither of the time-lapse sections (P-impedance and the time-lapse V_P/V_S) gives a clear response, then we do not need to perform interpretation because this area is marginally to not at all affected by the production.

Figure 3b shows the interpreted horizons for the field of our case study. When picking the tops and bases of the steam chambers, care must be taken not to make any misinterpretations because these will have a strong effect on the final results.

Updating the time-lapse low frequencies to map reservoir changes

After picking of the tops and bases of the production-affected zones, the contrasts in P-impedance and V_P/V_S are extracted over the interpreted horizons. This is done by measuring the extreme values directly above and below the interpreted horizons and subtracting them to form the contrasts. Linear interpolation between the contrasts is used to create the values for the time-lapse low-frequency model within the production-affected zones. Outside of the affected areas, the model values are zero. The simple interpolation of the contrast values in order to get the values within the production-affected zones is not a bad approximation because this model will be used only to fill in the missing time-lapse low frequencies, i.e., lower than 10 to 15 Hz. The time-lapse low-frequency models of P-Impedance and V_P/V_S are shown in Figure 3c.

Finally, the band-limited time-lapse model (Figure 3a) is merged with the time-lapse low-frequency model (Figure 3c) to build a new full-bandwidth time-lapse model. Figure 3d shows the final result of this updating procedure for one section in this heavy-oil field. The full-bandwidth elastic model can now be used to quantify production variations within the steam chambers.

Petroelastic template for steaming effects on elastic properties

The different behavior of the time-lapse P-impedance and V_P/V_S has been modeled based on well logs, seismic, and production data. The P-impedance and V_P/V_S responses can vary based on the production phase and the reservoir temperature.

Figure 4 shows the template linking elastic-property changes and temperature changes for this heavy-oil field. Different behaviors of P-impedance and V_P/V_S clearly

Reservoir pressure	3000 kPa											
Time steps	0	1	2	3	4	5	6	7	8	9	10	11
Temperature (deg C)	16	36.25	39	46	51.25	75	112.6	169.4	234.4	244	250	270
S_w	0.45	0.35	0.35	0.36	0.365	0.38	0.41	0.47	0.47	0.52	0.55	0.55
S_{oil}	0.55	0.65	0.65	0.64	0.635	0.62	0.59	0.53	0.22	0.21	0.2	0.2
$S_{gas}(1 - S_o - S_w)$	0	0	0	0	0	0	0	0	0.31	0.27	0.25	0.25
	Pre-steam reservoir	Bitumen becomes mobile but no production			Bitumen is mobilized. Production in progress. Brine replaces HC.				Production in progress. Vapor/chemical gases released from bitumen and replace HC.			Production is finished (final oil recovery); temperature just increases.

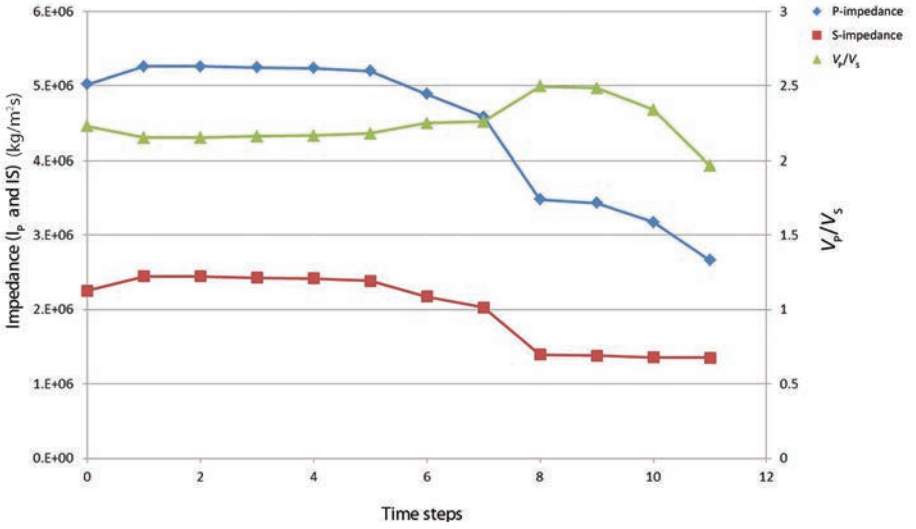

Figure 4. Rock-physics template showing the relationship between P-impedance and V_P/V_S with changes in the reservoir temperature at different production phases in different time steps. The reservoir life cycle is divided into 12 time steps, from cold reservoir (0) to depleted reservoir (11).

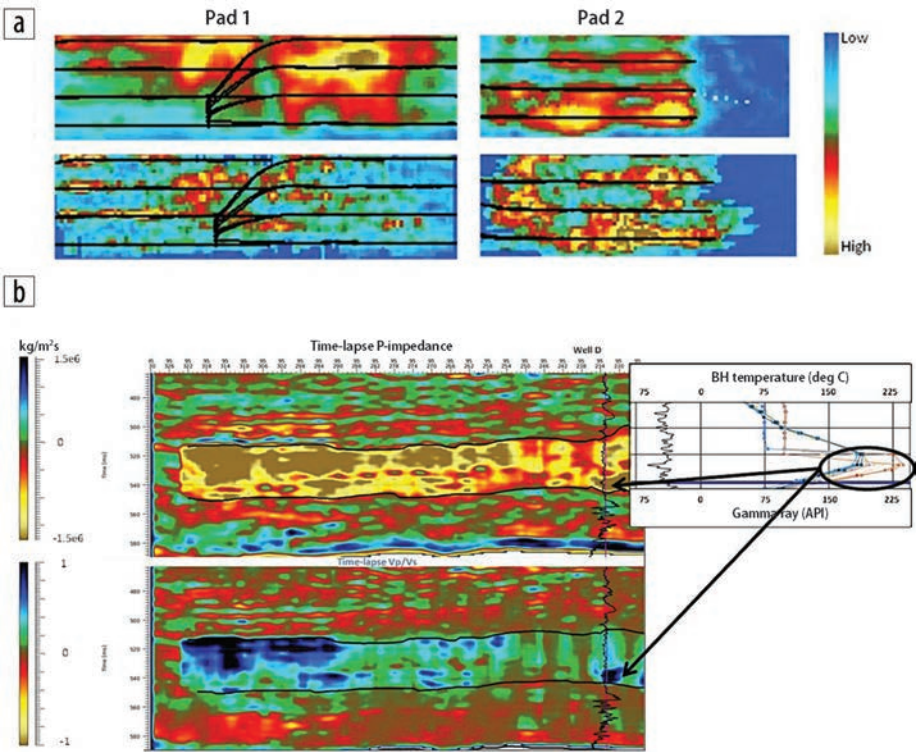

Figure 5. Comparison between inversion results and two independent sources of information. (a) Comparison with time-shift map on two well pads. The top images in part (a) are time-shift maps from a horizon below the reservoir, and the bottom ones are mean time-lapse P-impedance within the reservoir. (b) Comparison of time-lapse P-impedance (top) and time-lapse V_P/V_S (bottom) with temperature log at control well D close to a steam chamber. Refer to Figure 4 for the relationship between temperature and elastic properties.

are observed for different time steps, indicating a different production phase as well as a change in reservoir temperature.

Validation of results and discussion

The inversion results can be compared with other independent sources of information from this field. This comparison is necessary to validate our results as well as the proposed workflow for updating the low-frequency model. The rock-physics template given in Figure 4 is used to interpret the inversion results for validation purposes.

Figure 5 shows the comparison between the results from inversion and time-shift sections and temperature measurements at control wells close to the steam chambers. In particular, Figure 5a shows the comparison with time-shift measurements obtained in the time-alignment process. Time-shift maps of a horizon directly below the reservoir section are compared with average time-lapse P-impedance over the reservoir. The time-shift maps are indicative of velocity changes in the reservoir, whereas the P-impedance incorporates both velocity and density changes. Comparison of the two maps highlights areas with high correlation, indicating that the reservoir changes are dominated by velocity effects. Areas with little correlation indicate that effects of density and velocity changes probably cancel each other.

Figure 5b compares our results against temperature measurements in a control well close to the steam chambers. Because the elastic-parameter changes in the reservoir are dominated by temperature effects, there should be good correlation between inversion results and temperature measurements. Here, the upper section shows P-impedance changes, and the lower one depicts V_P/V_S changes. At the location of control well D, a decrease in P-impedance and an increase in V_P/V_S result from inversion. This elastic behavior is consistent with our petroelastic model for areas where the temperature increases from 160°C to 235°C. These results are also in agreement with temperature measurements in control well D, close to the steam chamber. This well is shown on both sections, and the temperature log is shown alongside.

Conclusions

Our method for updating time-lapse low-frequency models in a data-driven manner for time-lapse inversion studies has proved successful in its implementation on a heavy-oil reservoir produced using the SAGD method. The method is based on inversion of seismic differences and makes no assumptions about the reservoir conditions or about the relationships between elastic parameters. Our final results, based on the updated low-frequency models, are confirmed by independent information. Therefore, we can claim that our inversion workflow, when used in conjunction with the appropriate petroelastic model, may provide a robust approach for quantitative reservoir characterization of production parameters such as temperature and pressure. TLE

Acknowledgments

We thank our client for giving us the necessary permission to present the results shown in the figures. We also thank CGG for permission to publish this work.

Corresponding author: Reza.Saberi@CGG.com

References

Mesdag, P. R., D. Marquez, L. de Groot, and V. Aubin, 2010, Low frequency trend modeling for quantitative characterization of subsalt reservoirs: 72nd Conference and Exhibition, EAGE, Extended Abstracts, F027, http://dx.doi.org/10.3997/2214-4609.201400777.

Michou, L., Y. Lafet, T. Coleou, and J. Przybysz-Jarnut, 2013, 4D seismic inversion on continuous land seismic reservoir monitoring of thermal EOR: 75th Conference and Exhibition, EAGE, Extended Abstracts, http://dx.doi.org/10.3997/2214-4609.20130427.

Sarkar, S., W. P. Gouveia, and D. H. Johnston, 2003, On the inversion of time-lapse data: 73rd Annual International Meeting, SEG, Expanded Abstracts, 1489–1492, http://dx.doi.org/10.1190/1.1817575.